Article

Cell Reports

Yap1 Regulates Multiple Steps of Chondrocyte Differentiation during Skeletal Development and Bone Repair

Graphical Abstract

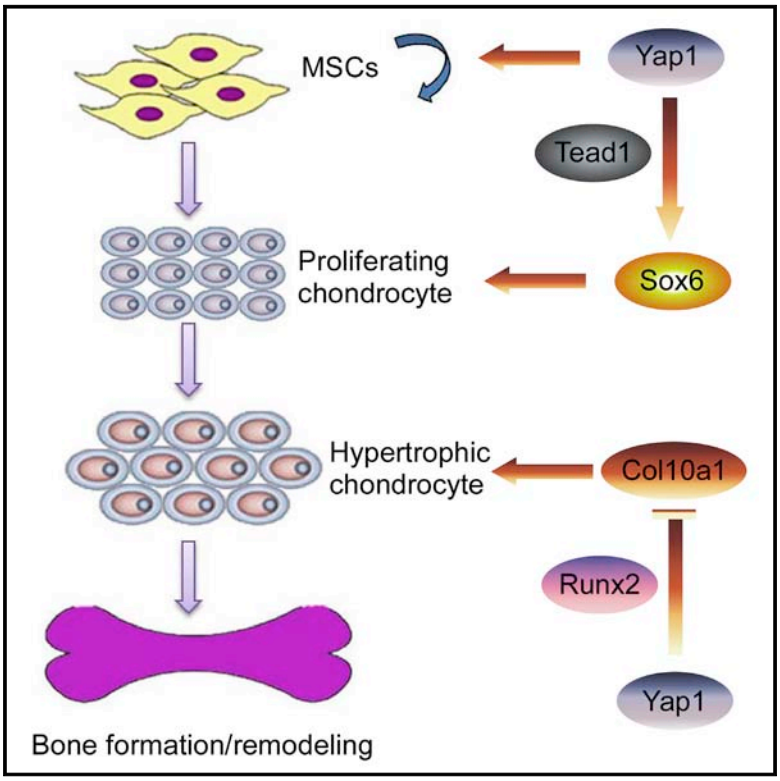

Authors

Yujie Deng, Ailing Wu, Pikshan Li, Gang Li, Ling Qin, Hai Song, Kinglun Kingston Mak

Correspondence

kmak@cuhk.edu.hk

In Brief

Deng et al. show that *Yap1* differentially regulates chondrocyte differentiation in both skeletal development and bone repair. *Yap1* requires *Teads* binding for direct regulation of *Sox6* expression to promote early chondrocyte proliferation. *Yap1* inhibits *Col10a1* expression through interaction with *Runx2* during chondrocyte maturation.

Highlights

- The expression of *Yap1* gradually decreases during chondrocyte maturation
- *Yap1* inhibits skeletal development, postnatal growth, and bone repair
- *Yap1* promotes early chondrocyte proliferation but inhibits subsequent maturation
- Sox6 *and Col10a1* are downstream targets regulated by *Yap1*

Deng et al., 2016, Cell Reports *14*, 1–14
March 15, 2016
http://dx.doi.org/10.1016/j.celrep.2016.02.021

CellPress

Please cite this article in press as: Deng et al., Yap1 Regulates Multiple Steps of Chondrocyte Differentiation during Skeletal Development and Bone Repair, Cell Reports (2016), http://dx.doi.org/10.1016/j.celrep.2016.02.021

Cell Reports
Article

Yap1 Regulates Multiple Steps of Chondrocyte Differentiation during Skeletal Development and Bone Repair

Yujie Deng,[2] Ailing Wu,[7] Pikshan Li,[6] Gang Li,[4] Ling Qin,[5] Hai Song,[7] and Kinglun Kingston Mak[1,2,3,*]
[1]Ministry of Education Key Laboratories for Regenerative Medicine, School of Biomedical Sciences, Faculty of Medicine, The Chinese University of Hong Kong, Shatin, Hong Kong SAR, China
[2]Stem Cell and Regeneration Thematic Research Program, School of Biomedical Sciences, The Chinese University of Hong Kong, Shatin, Hong Kong SAR, China
[3]School of Biomedical Sciences Core Laboratory, Shenzhen Research Institute, The Chinese University of Hong Kong, Shenzhen 518057, China
[4]Stem Cells and Regeneration Medicine Laboratory, Department of Orthopaedics & Traumatology, Li Ka Shing Institute of Health Sciences, Faculty of Medicine, The Chinese University of Hong Kong, Shatin, Hong Kong SAR, China
[5]Musculoskeletal Research Laboratory, Department of Orthopaedics & Traumatology, Faculty of Medicine, The Chinese University of Hong Kong, Shatin, Hong Kong SAR, China
[6]Transgenic Core, The Chinese University of Hong Kong, Shatin, Hong Kong SAR, China
[7]Life Sciences Institute and Innovation Center for Cell Signaling Network, Zhejiang University, Hangzhou 310058, China
*Correspondence: kmak@cuhk.edu.hk
http://dx.doi.org/10.1016/j.celrep.2016.02.021

SUMMARY

Hippo signaling controls organ size and tissue regeneration in many organs, but its roles in chondrocyte differentiation and bone repair remain elusive. Here, we demonstrate that *Yap1*, an effector of Hippo pathway inhibits skeletal development, postnatal growth, and bone repair. We show that *Yap1* regulates chondrocyte differentiation at multiple steps in which it promotes early chondrocyte proliferation but inhibits subsequent chondrocyte maturation both in vitro and in vivo. Mechanistically, we find that *Yap1* requires *Teads* binding for direct regulation of *Sox6* expression to promote chondrocyte proliferation. In contrast, *Yap1* inhibits chondrocyte maturation by suppression of *Col10a1* expression through interaction with *Runx2*. In addition, *Yap1* also governs the initiation of fracture repair by inhibition of cartilaginous callus tissue formation. Taken together, our work provides insights into the mechanism by which *Yap1* regulates endochondral ossification, which may help the development of therapeutic treatment for bone regeneration.

INTRODUCTION

Endochondral ossification is an important process for both skeletal development and bone repair. In the long bones, cartilage anlage is first formed by mesenchymal condensation, followed by chondrocyte differentiation and maturation and subsequently bone mineralization (Kronenberg, 2003). Similarly, bone repair employs similar mechanism to regenerate new bone tissues after injury (Bolander, 1992; Bruder et al., 1994; Deschaseaux et al., 2009; Einhorn, 1998; Ferguson et al., 1999; Wang and Boyapati, 2006). For instance, during fracture healing, mesenchymal stem cells (MSCs) migrate to the wound site and differentiate into chondroblasts and chondrocytes. These cells then undergo proliferation, hypertrophy, and mineralization to form cartilaginous callus tissues. New bone is then deposited, and the process is completed through bone remodeling that restores normal shape and function of the bones. These sequential steps are concomitantly regulated by key transcription factors that are highly conserved during skeletal development. *Sox9* is a major regulator for early chondrogenesis (Lefebvre and de Crombrugghe, 1998). It promotes chondrocyte differentiation and cooperatively interacts with transcriptional factors *Sox5* and *Sox6* for chondrocyte proliferation and differentiation (Akiyama et al., 2002; Smits et al., 2001). Chondrocyte matrix components such as Aggrecan and Col2a1 are then sequentially expressed (Han and Lefebvre, 2008; Lefebvre et al., 1998). *Runx2*, a major regulator of chondrocyte hypertrophy (Takeda et al., 2001), subsequently expressed and regulates the expression of its target genes such as *Col10a1* for successive chondrocyte maturation (Zheng et al., 2003). Many signaling pathways are implicated in the chondrocyte differentiation process to tightly regulate the pace of cartilage and bone formation during skeletal development and fracture healing. For instance, Ihh (Vortkamp et al., 1998), Pth (Ellegaard et al., 2010), Bmp (Tsuji et al., 2006), and Wnt/β-catenin (Huang et al., 2012) signaling all contribute to both processes. However, bone repair is not as efficient as skeletal development by activation of these pathways suggesting that the regulatory mechanisms for these processes are more complicated than expected and additional signaling interactions may be involved for the process.

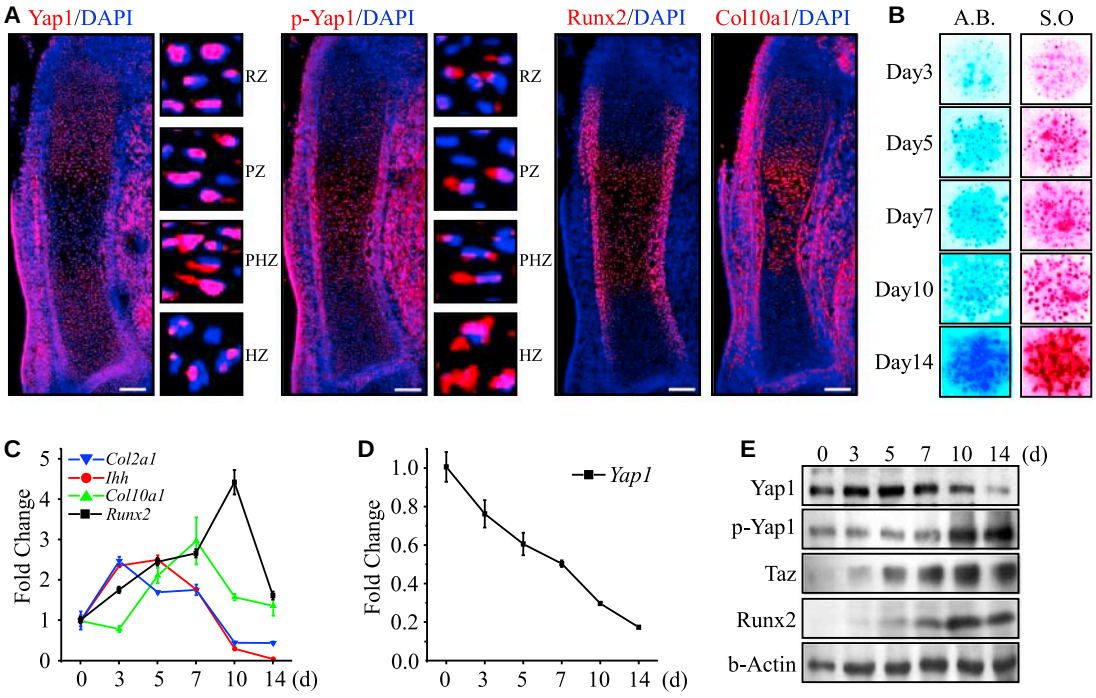

Figure 1. *Yap1* Expression Is Gradually Reduced during Chondrocyte Differentiation

(A) Yap1 was expressed in the growth plates of wild-type tibias at E14.5 (n = 3 per group) as shown by immunofluorescence (RZ, resting chondrocytes; PZ, proliferative chondrocytes; PHZ, prehypertrophic chondrocytes; HZ, hypertrophic chondrocytes). Scale bars, 100 μm. See also Figure S1.

(B) Micromass culture from chondroprogenitor cells isolated from E12.5 wild-type embryos. Cultures were stained with Alcian blue (A.B.) and Safranin O (S.O.) solution as shown.

(C and D) Gene expression analysis of micromass culture from (B).

(E) Protein analysis of micromass culture from (B). The experiment was repeated three times independently. Error bars represent SD.

Hippo signaling controls organ size (Pan, 2007; Song et al., 2010; Wu et al., 2003; Zhou et al., 2009) and tissue regeneration in many organs (Heallen et al., 2013; Karpowicz et al., 2010; Zhao et al., 2011). Central to this pathway is a kinase cascade consisting of Mst1/2, Sav, Lats1/2, and Mats in the mammalian system. When the Hippo signaling is active, a series of phosphorylation events via Msts and Lats kinases occurs and ultimately leads to the phosphorylation of Yap1, a key effector of the pathway (Halder and Johnson, 2011; Pan, 2010; Zhao et al., 2010). Phosphorylated Yap1 is sequestered in the cytoplasm, which inhibits its transcriptional activity. In contrast, inactivation of the Hippo pathway increases Yap1 nuclear translocation. It then interacts with *Tead/Tef* family transcription factors to activate Hippo target genes that are responsible for cell proliferation and apoptosis. Other than *Teads*, it has been recently shown that Yap1 is also able to interact with many other transcription factors for the crosstalk with different signaling pathways (Alarcón et al., 2009; Espanel and Sudol, 2001; Fernandez-L et al., 2009; Rosenbluh et al., 2012), suggesting that Yap1 serves as a regulator to integrate multiple signaling cascades during many biological processes. In the context of the bone, Zaidi et al. previously showed that Yap1 mediated by Src/Yes tyrosine kinase signaling interacts with *Runx2* to regulate *Osteocalcin* expression (Zaidi et al., 2004). In vitro studies also demonstrate that *Yap1* inhibits osteogenesis from bone-marrow-derived MSCs (Seo et al., 2013). In contrast, high *Yap1* activities in MSCs promote osteogenesis (Dupont et al., 2011). However, whether Hippo signaling or *Yap1* regulates chondrocyte differentiation and bone repair remain largely unclear.

Here, we investigated the roles of *Yap1* in regulating chondrocyte differentiation and maturation during skeletal development, postnatal growth, and bone repair. We found that *Yap1* promotes early chondrocyte proliferation but inhibits chondrocyte hypertrophy and maturation both in vitro and in vivo, but its effect is more pronounced during bone repair. Specifically, *Yap1* attenuates endochondral ossification during both skeletal development and fracture healing. Our findings provide insights into the regulatory mechanisms in chondrocyte differentiation for bone formation and repair.

RESULTS

Yap1 Expression Gradually Reduces during Chondrocyte Differentiation

To study the roles of *Yap1* during skeletal development, we first examined the endogenous expression pattern of Yap1 in the long bones during endochondral bone formation. In the growth plates of mouse embryos, we found that Yap1 was expressed in resting and proliferative chondrocytes but less in hypertrophic chondrocytes at E14.5 (Figures 1A and S1). In contrast, the expression of phosphorylated Yap1 was strongest in the hypertrophic chondrocytes where *Col10a1* and *Runx2* expression

were detected. It suggests that Yap1 activity was gradually reduced during chondrocyte maturation. We also performed micromass culture using chondroprogenitor cells isolated from the limb buds of E12.5 wild-type embryos (Figure 1B). During chondrocyte differentiation, chondrocyte markers such as *Col2a1*, *Ihh*, and *Col10a1* were increased and peaked at around day 5 to day 7 and then gradually reduced thereafter (Figure 1C). *Runx2* expression was peaked at day 10. Interestingly, Yap1 expression was gradually reduced along with cartilage nodule formation while the expression level of phosphorylated Yap1 was gradually increased (Figures 1D and 1E). These expression patterns were consistent with the expressions observed in the growth plates. We also examined the expression pattern of *Yap1* paralog *Taz* (Figure 1E). However, its expression was gradually increased during cartilage nodule formation in micromass culture, which was opposite to that of total Yap1 expression. Altogether, both in vivo and in vitro data suggest that Yap1 plays a functional role in regulating chondrocyte differentiation.

Yap1 Inhibits Skeletal Development and Postnatal Growth

To examine the functional roles of *Yap1* in vivo, we generated transgenic mice in which *Yap1* was overexpressed in chondrocytes as well as osteoprogenitor cells under the control of *Col2a1* promoter and enhancer (Long et al., 2001). Two transgenic lines (TG01 and TG02) were generated (Figure S2A), and both of them showed Yap1 overexpression in all chondrocytes, but not other tissues being tested (Figures S2B–S2E). Since TG01 displayed a higher level of *Yap1* expression and therefore it was selected for subsequent analyses and named as *Col2a1-Yap1*$^{tg/+}$. Surprisingly, the *Col2a1-Yap1*$^{tg/+}$ transgenic mice showed mild skeletal abnormalities at birth with the skeleton of normal size and shape as compared to that of the control littermates (Figure 2A), suggesting that endochondral bone formation was largely unaffected. The subtle phenotypes during early skeletal development suggest that the developing skeleton is either insensitive to *Yap1* overexpression or the overexpression level of *Yap1* is not strong enough. We therefore further increased *Yap1* overexpression by self-crossing the *Col2a1-Yap1*$^{tg/+}$ transgenic line to generate a homozygous *Col2a1-Yap1*$^{tg/tg}$ transgenic mice (Figure S2F). The transgene copy number was doubled in the homozygous transgenic mice (Figure S2G), and the expression of Yap1 in chondrocytes was much stronger than that of the heterozygous *Col2a1-Yap1*$^{tg/+}$ transgenic mice (Figures S2H–S2J) while the expression of *Taz* was unaffected (Figure S2H). Interestingly, only homozygous *Col2a1-Yap1*$^{tg/tg}$ transgenic chondrocytes showed a significant upregulation of Hippo target genes *Cyr61* and *Ctgf*, albeit a trend of increase expression was observed in the heterozygous group (Figures S2I and S2J). This may explain the mild skeletal phenotypes observed in the *Col2a1-Yap1*$^{tg/+}$ transgenic mice. The homozygous *Col2a1-Yap1*$^{tg/tg}$ transgenic mice displayed a markedly smaller skeleton size than that of the heterozygous transgenic mice (Figure 2A). Close histologic examination of the long bones revealed that all the chondrocyte zones were present in the transgenic groups and the overall length of the growth plates was progressively shorter with increasing Yap1 overexpression (Figure 2B). Similar results were observed in the vertebral columns (Figure S2K). Next, we examined the maturation of terminally differentiated hypertrophic chondrocytes by von Kossa staining (Figures 2C and S2L). Both the growth plates from the long bones and the vertebral columns displayed reduction of mineralization of hypertrophic chondrocytes at the chondro-osseous junctions. Consistently both Col10a1 and Mmp13 expression were also reduced in the long bone sections (Figures 2D and 2E). These data suggest that chondrocyte hypertrophy was delayed in vivo and that Yap1 inhibits chondrocyte maturation during skeletal development.

We asked whether postnatal skeletal growth of the *Col2a1-Yap1* transgenic mice was also affected. We observed that the secondary ossification center in the long bones of the *Col2a1-Yap1*$^{tg/tg}$ transgenic mice was delayed starting from 1 week of age (Figure 2F). Subchondral bone region was also significantly smaller at 4 weeks old (Figure 2G). The overall bone mass accrual was significantly lower when compared with their age-matched wild-type littermates (Figures 2H and 2I). However, we cannot exclude the possibility that the phenotypes may be also in part contributed by osteoblasts as *Col2a1*$^{+}$ cells also expressed in early perichondrium. Altogether, our data suggest that *Yap1* inhibits endochondral ossification during skeletal development and growth.

To examine whether *Yap1* is required for skeletal development and bone growth, we generated *Yap1*$^{c/c}$*;Col2a1-Cre* mutant mice. Skeletal preparation at both E16.5 and E18.5 showed that the *Yap1*$^{c/c}$*;Col2a1-Cre* mutant mice was slightly bigger in size than that of the age-matched wild-type littermates (Figures 3A–3H). Mild increases of mineralized tissues were observed. Histologic examinations revealed that the mutant growth plates were progressively longer than that of the controls with age (Figures 3I, 3K, and 3M). The expression of hypertrophic markers Col10a1 and Runx2 were increased in the mutant growth plates (Figure 3J), and mineralization was also significantly increased as revealed by von Kossa staining (Figures 3L and 3N). These data mirrored the phenotypes of the *Col2a1-Yap1*$^{tg/tg}$ transgenic mice. Altogether, our data strongly indicate that *Yap1* inhibits chondrocyte maturation and endochondral ossification during bone development.

Yap1 Promotes Early Chondroprogenitor Cell Proliferation

To investigate the mechanistic actions of *Yap1* during chondrocyte differentiation and maturation, we first examined its roles in early events of chondrogenesis by manipulating *Yap1* expression in MSCs isolated from mouse bone marrows with lentiviruses (Figures S3A–S3C). The proliferation rate of MSCs was greatly increased when *Yap1* was overexpressed for 72 hr as revealed by MTT assay (Figure 4A). Colony formation assay also showed a significant increase of the number of colonies (Figures 4B and 4C). Gene expression of stemness markers such as *Sox2*, *Pou5f1*, and *Klf4* were all significantly upregulated (Figure 4D). In contrast, knockdown of *Yap1* displayed mirror phenotypes of the overexpression studies (Figures 4E–4H). We also performed the colony formation assay using chondroprogenitor cell line ATDC5, and consistent results were obtained (Figures S3D and S3E). These results indicate that *Yap1* is required for chondroprogenitor cell proliferation and maintenance. Similarly,

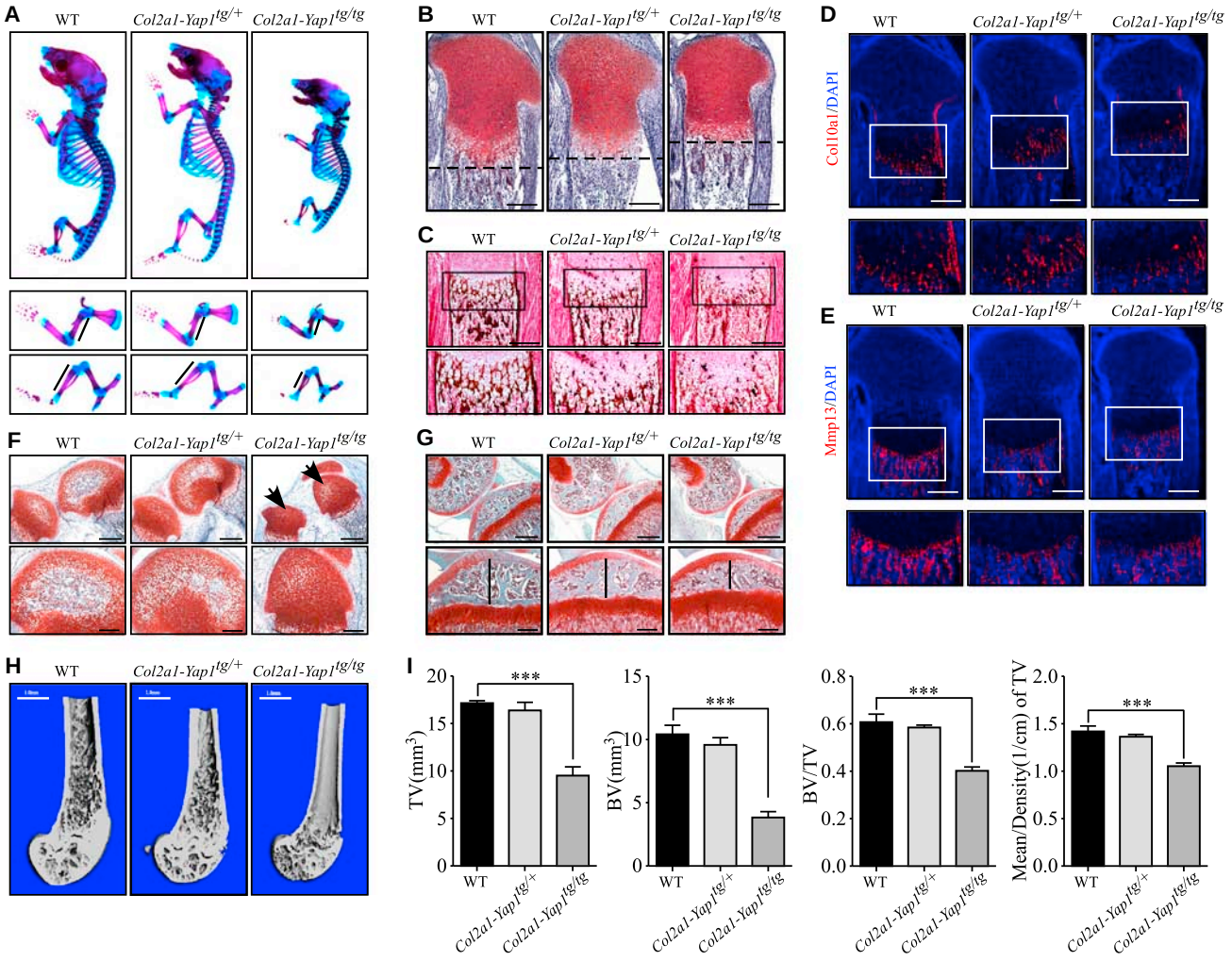

Figure 2. Skeletal Abnormalities of *Col2a1-Yap1* Transgenic Mice

(A) Skeletal preparations of newborn mice (n = 3 per group) with respective genotypes at postnatal day 1 as shown. Forelimb and hind limb are shown in the lower panel with higher magnification. See also Figure S2.

(B) Growth plate sections of the tibia of respective mice (n = 6 per group) at day 1 as shown by Safranin O staining. Scale bars, 250 μm. See also Figures S2K and S2L.

(C) Terminally differentiated hypertrophic chondrocytes in tibias of respective mice (n = 6 per group) are shown by von Kossa staining at day 1. Boxed areas showed the regions with reduction of calcification of terminally differentiated hypertrophic chondrocytes in the transgenic groups. Scale bars, 250 μm.

(D and E) Immunohistochemistry of tibial growth plates of (D) Col10a1 and (E) Mmp13 expression of respective mice (n = 3 per group) as shown. Boxed region showed higher magnification of expression patterns. Scale bars, 250 μm.

(F) Safranin O staining of femoral secondary ossification centers at day 10 of mice with respective genotypes as shown. Scale bars, 500 μm (upper panel); 250 μm (lower panel). Arrows point to the regions of secondary ossification centers.

(G) Tibial subchondral bone regions of respective genotypes as shown by Safranin O staining at day 28 (n = 3 per group). The length of the epiphysis was indicated by black bars. Scale bars, 500 μm (upper panel); 250 μm (lower panel).

(H) 3D micro-CT images of the femur of 10-week-old mice (n = 3 per group). Scale bars, 1 mm.

(I) Histomorphometric analysis of bone parameters in the femur of mice in (H). Error bars represent SD (***$p < 0.001$).

knockdown of *Taz* also showed consistent results in cell proliferation and colony formation as in *Yap1* knockdown (Figures S3F–S3K). It suggests that both *Yap1* and *Taz* play similar roles in regulating early chondroprogenitor cell proliferation. In addition, *Yap1*$^{c/c}$*;Prx1-Cre* mutant mice, in which *Yap1* was removed in early limb bud mesenchyme, also displayed a significant smaller skeleton (Figures S3L–S3N). This is mainly a consequence of reduced proliferation of early chondroprogenitor cells. Taken together, our data indicate that *Yap1* plays a positive role in regulating early chondroprogenitor cell proliferation.

Yap1 Promotes Chondrocyte Proliferation by Regulation of *Sox6* Expression through *Teads* Binding

Next, we investigate the roles of *Yap1* in chondrocyte proliferation by examining phosphohistone-3 (PH-3) expression in the *Col2a1-Yap1* transgenic mice. Interestingly, chondrocyte

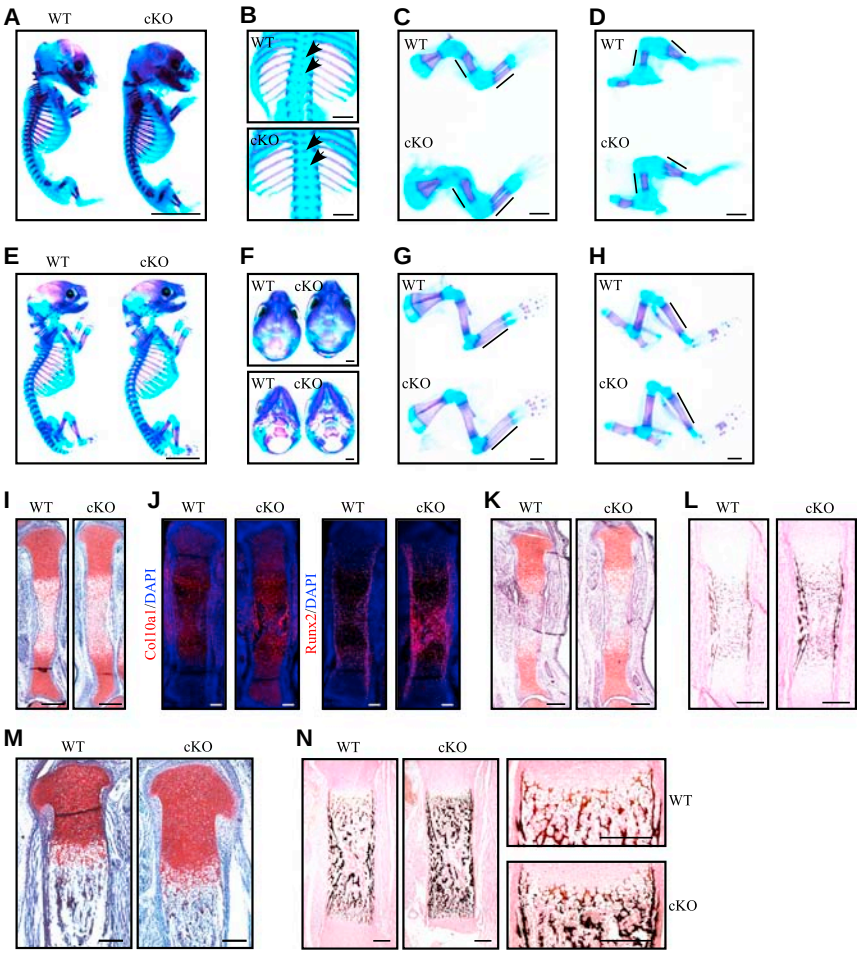

Figure 3. Skeletal Phenotypes of *Yap1*$^{c/c}$; *Col2a1-Cre* Mutant Mice

(A–H) Skeletal preparations of mice at (A–D) E16.5 and (E–H) E18.5 with genotypes as shown. Arrows and black bars show regions with increased mineralization. Scale bars, 5 mm for the whole skeleton; 1 mm for individual region.

(I–N) Tibial growth plates of (I)–(J) at E15.5, (K)–(L) E16.5, and (M) and (N) E18.5 with genotypes as shown. Scale bars, 250 μm (I, K, and N); 100 μm (J); and 200 μm (L and M).

proliferation was increased in the growth plates of both transgenic groups (Figures 5A and 5B). Similar results were obtained in the primary chondrocytes isolated from the transgenic mice as well (Figures 5C and 5D). To understand the targets regulated by *Yap1* during chondrocyte proliferation, we search for genes involved in the regulation of chondrocyte proliferation. *Sox6* is reported to be responsible for regulating chondrocyte proliferation (Smits et al., 2001), and we found multiple tentative *Tead* binding sites in the promoter region of *Sox6* (Figure 5E). *Teads* are transcriptional factors required for Yap1 binding to DNA (Vassilev et al., 2001). We therefore performed chromatin immunoprecipitation (ChIP) assay using primary chondrocytes isolated from the *Col2a1-Yap1*$^{tg/+}$ transgenic mice. DNA of the specific *Tead* binding regions was amplified after immunoprecipitation with Yap1 antibodies. A strong PCR band was detected in the BS2 region of the *Sox6* promoter (Figure 5F), suggesting that *Yap1/Teads* complexes induce *Sox6* expression. To confirm this finding, we examined *Sox6* expression in the *Col2a1-Yap1*$^{tg/+}$ transgenic chondrocytes isolated from the growth plates of the long bones. As expected, transgenic chondrocytes displayed strong upregulation of *Sox6* expression (Figure S4A). Similarly, we overexpressed *Yap1* in primary chondrocytes and found that the expression of *Sox6* was upregulated (Figure 5G). In contrast, knockdown of *Yap1* resulted in a significant reduction of *Sox6* expression (Figure 5H). Furthermore, dual luciferase assay using reporter plasmids with promoter region 1.2 kb upstream of the transcription start site of *Sox6* showed consistent results with both *Yap1* overexpression and knockdown studies (Figures 5I–5J). Knockdown of *Sox6* in primary chondrocyte of *Col2a1-Yap1*$^{tg/+}$ transgenic mice (Figure S4B) displayed significantly reduced chondrocyte proliferation (Figures 5K and S4C). Similarly, knockdown of *Yap1* also showed reduced chondrocyte proliferation (Figures 5L, S4D, and S4E). However, when *Sox6* was overexpressed, the reduced chondrocyte proliferation was rescued to a similar level as in the control. These findings indicate that *Yap1* mediates its effect at least in part through *Sox6* in promoting chondrocyte proliferation.

In order to test whether the effect of *Yap1* on *Sox6* expression is dependent on *Teads* binding, we overexpressed a mouse *Yap1S79A* mutant (same mutation as human *Yap1S94A*) in chondrocytes in which the binding site with Teads was mutated. The effects of *Yap1* on *Sox6* expression were abolished in both the RNA and protein levels when mutant Yap1S79A was expressed (Figures 5M, 5N, and S4F). Dual luciferase assay using the same *Sox6* reporter plasmids also showed a significant reduction of luciferase activities similar to the background level (Figure 5O). In addition, ChIP assay revealed that the enrichment of BS2 region of the *Sox6* promoter was significantly reduced with *Yap1S79A* (Figure 5P). These data indicate that *Teads* binding is necessary for *Yap1* to regulate *Sox6* expression. Collectively, our results indicate that *Yap1* promotes early chondrocyte proliferation through regulation of *Sox6* expression in a *Teads*-dependent manner.

Yap1 Inhibits Chondrocyte Maturation by Regulation of *Col10a1* Expression through *Runx2* Interaction

Although early cell proliferation was increased by *Yap1* overexpression, the growth plates of *Col2a1-Yap1* transgenic groups were significantly smaller as compared to their respective controls suggesting that chondrocyte maturation was remarkably

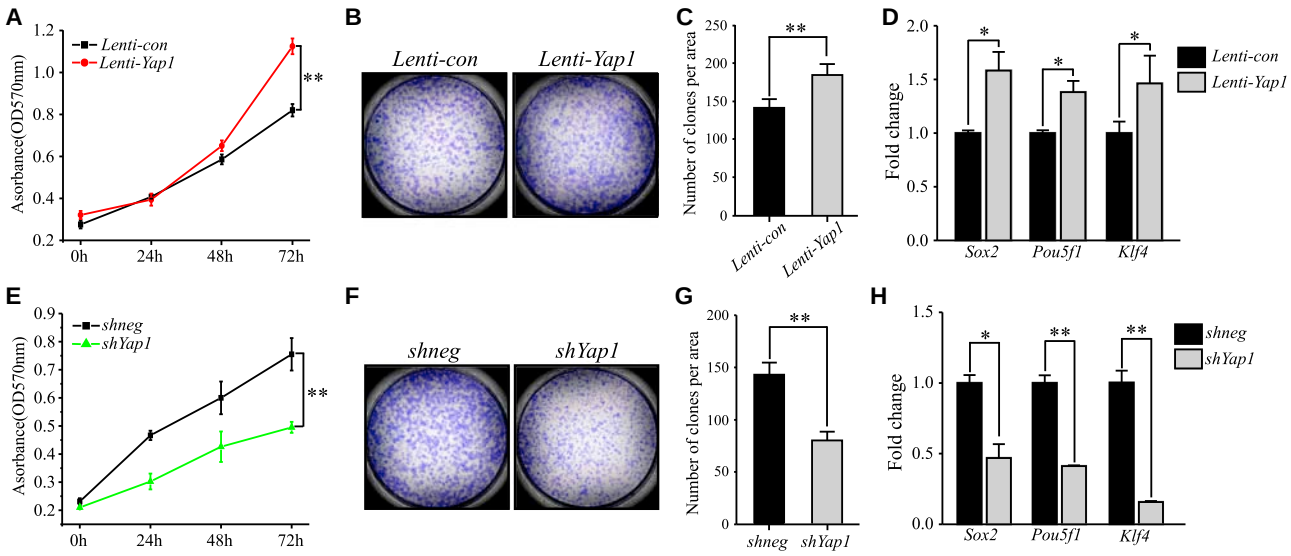

Figure 4. *Yap1* Promotes Chondroprogenitor Cell Proliferation and Is Required for Its Maintenance

(A) Cell proliferation rate of bone marrow MSCs as shown by MTT assay after 72 hr. See also Figure S3.

(B) Colony formation assay of mouse bone marrow MSCs as shown by crystal violet staining.

(C) Statistical analysis of colony numbers from (B).

(D) Gene expression analysis using samples from (A).

(E) Cell proliferation rate of bone marrow MSCs with sh*Yap1 lentiviruses* as shown by MTT assay.

(F) Colony formation assay with *shYap1*.

(G) Statistical analysis of (F).

(H) Gene expression analysis using samples from (E). The qRT-PCR analysis was performed in triplicates and repeated three times independently. Error bars represent SD (**p < 0.01; *p < 0.05).

impaired. To further confirm the phenotypes, we isolated limb bud cells from the *Col2a1-Yap1*$^{tg/+}$ transgenic embryos and performed micromass culture. We found that cartilage nodule formation and maturation was greatly delayed at day 7 (Figure S5A). The delay was more pronounced at day 14. Gene expression of *Col2a1*, *Aggrecan*, and *Col10a1* were all significantly downregulated (Figure S5B) indicating that chondrocyte maturation was inhibited. Micromass culture using wild-type limb bud cells with *Yap1 adenovirus* infection showed similar results (Figures 6A, 6B, S5C, and S5D). In contrast, knockdown of *Yap1* increased cartilage nodule formation, and all chondrocyte markers being examined were upregulated (Figures 6C and 6D). Consistently, micromass culture using ATDC5 cell line also showed similar results (Figures S5E–S5H). Taken together, our results indicate that *Yap1* inhibits chondrocyte differentiation and maturation both in vivo and in vitro. However, knockdown of *Taz* in micromass culture showed slower maturation (Figure S5I). Chondrocyte maturation markers were all downregulated in micromass culture as well as in primary chondrocytes with *shTaz* transduction (Figures S5J and S5K). In contrast, *Taz* overexpression in primary chondrocytes increased their expressions (Figure S5L). These data indicate that *Yap1* and *Taz* function paradoxically opposite with each other in regulating chondrocyte maturation.

To identify the mechanistic roles of *Yap1* in inhibiting chondrocyte maturation, we first examined the expression of hypertrophic marker *Col10a1*. We found that overexpression of *Yap1* in primary chondrocytes inhibited *Col10a1* expression (Figure 6E), which was consistent with our in vivo results (Figure 2D). In contrast, knockdown of *Yap1* relieved the suppression of *Col10a1* expression (Figure 6F). It has been previously reported that *Runx2* is a key regulator for *Col10a1* expression and chondrocyte hypertrophy (Takeda et al., 2001) in which *Runx2* promotes *Col10a1* expression (Figure 6G). Thus, we overexpressed *Yap1* in the presence of *Runx2* in primary chondrocytes to examine the changes of *Col10a1* expression (Figure 6H). Similar to previous observations, *Yap1* overexpression inhibited *Runx2*-induced *Co10a1* expression. Next, we cloned a 1.5-kb promoter region upstream of the transcription start site of *Col10a1* to the luciferase reporter plasmids for dual luciferase assay. We showed that *Runx2* expression resulted in a dose-dependent increase of the luciferase activities in our *Co10a1* reporter plasmids in wild-type primary chondrocytes (Figure 6I). In agreement with our previous results, *Yap1* overexpression in primary chondrocytes inhibited luciferase activities of *Col10a1*, while knockdown of *Yap1* enhanced it (Figure 6J). When we co-transfected *Runx2* with *Yap1*, the *Runx2*-induced luciferase activities of *Col10a1* was suppressed (Figure 6K). Further increase of *Yap1* expression revealed a dose-dependent inhibitory effect (Figure 6L). In contrast, when *Yap1* was knocked down, the *Col10a1* luciferase activities were further enhanced as compared to the *Runx2* alone group (Figure 6K). Similarly, we repeated these experiments using 293T cell lines and consistent results were obtained (Figures S6A and S6B). Furthermore,

increased expression of *Runx2* was able to rescue the inhibitory effects of *Yap1* (Figure S6C). We also showed that Runx2 co-localized with Yap1 in primary chondrocytes (Figure 6M). Immunoprecipitation with Yap1 antibodies also displayed positive interaction of Runx2 in primary chondrocytes (Figure 6N). Reciprocally, pull-down of Runx2 revealed a positive interaction with Yap1 (Figure 6O). Next, we determined whether the binding of Runx2 with Yap1 requires Teads. Interestingly, immunoprecipitation assay showed that *Tead1* overexpression significantly reduced the binding of Yap1 with Runx2 (Figure S6D). This suggests that Runx2 competes with Teads for Yap1 interaction during maturation. We further performed a ChIP assay in the promoter region of *Col10a1* where three *Runx2* binding sites were found (Figure 6P) (Li et al., 2011; Zheng et al., 2003). ChIP assay using Runx2 antibodies revealed that *Yap1* overexpression reduced the enrichment of PCR bands in BS-2 and BS-3 (Figure 6Q). It suggests that Yap1 competes for Runx2 and releasing Runx2 from chromatin. Interestingly, increasing expression of *Taz* progressively induced the luciferase activities of *Col10a1* in the presence of *Runx2* (Figure S6E), which is in sharp contrast to *Yap1* function. Overexpression of *Taz* also enhanced the binding of Runx2 to BS-1 domain of the *Col10a1* promoter region (Figure 6Q). All these data indicate that *Taz* competes with *Yap1* for *Runx2* interaction in order to modulate the expression of *Col10a1* to control chondrocyte maturation. Altogether, our data indicate that *Yap1* inhibits chondrocyte maturation by regulating *Col10a1* expression through interaction with *Runx2*.

Yap1 Overexpression or Inactivation of Hippo Signaling Impairs Cartilaginous Callus Formation during Bone Repair

To gain further insights of *Yap1* in postnatal skeletal function and given that appropriate and controlled chondrocyte maturation play fundamental roles in the initial steps of bone repair, we therefore created standardized fractures in the *Col2a1-Yap1*$^{tg/+}$ transgenic mice and the *Mst1*$^{c/c}$*; Mst2*$^{c/c}$*; Dermo1-Cre* mutant mice, respectively (Figure 7). Both Mst1 and Mst2 kinases were genetically removed simultaneously at very early limb mesenchyme using *Dermo1-Cre* mouse line (Yu et al., 2003) that resulted in Yap1 activation as shown by reduced phosphorylated Yap1 (Figure S7A). Consistent with the *Col2a1-Yap1*$^{tg/+}$ transgenic mice, cell proliferation was significantly increased in the *Mst1*$^{c/c}$*; Mst2*$^{c/c}$ chondrocytes after *Cre adenovirus* infection (Figures S7B and S7C). Mild delayed of chondrocyte hypertrophy was observed in the long bones of the *Mst1*$^{c/c}$*; Mst2*$^{c/c}$*; Dermo1-Cre* mutant mice (Figures S7D and S7E). All the skeletal phenotypes in the *Mst1*$^{c/c}$*; Mst2*$^{c/c}$*; Dermo1-Cre* mutant mice strongly resembled to the heterozygous *Col2a1-Yap1*$^{tg/+}$ transgenic mice. Thus, we used both animal models to study bone repair. Two weeks after fracture injury, radiographs from wild-type mice showed obvious callus formation at the site of fracture with significant amount of cartilage formation (Figures 7A, 7B, 7G, and 7H). However, cartilaginous callus formation in the *Col2a1-Yap1*$^{tg/+}$ transgenic mice and the *Mst1*$^{c/c}$*; Mst2*$^{c/c}$*; Dermo1-Cre* mutant mice were significantly impaired (Figures 7A, 7B, 7G, and 7H). Only a residual amount of chondrocytes were observed as shown by Safranin O staining. Micro-CT analyses further revealed that both bone volume and bone surface of the callus tissues were significantly reduced (Figures 7E, 7F, 7J, and 7K). Histological sections showed that transgenic chondrocytes were less mature than that of the wild-type control as revealed by less Safranin O staining intensity (Figure 7B) and less proteoglycan contents as revealed by reduction of *Aggrecan* expression (Figure 7D). Sox9 expression level was largely unchanged in both immunohistochemistry and qRT-PCR analyses, but Col2a1 and Col10a1 expression was significantly reduced (Figures 7C and 7D). Similar gene expression pattern was also observed in the callus tissues isolated from the *Mst1*$^{c/c}$*; Mst2*$^{c/c}$*; Dermo1-Cre* mutant mice (Figure 7I), and the phenotypes were generally more severe as compared to that of the *Col2a1-Yap1*$^{tg/+}$ transgenic mice. Collectively, our data indicate that fracture healing is greatly impaired with *Yap1* overexpression due to early inhibition of cartilaginous callus formation during endochondral ossification.

DISCUSSION

Here, we present mechanistic functions of *Yap1* in regulating chondrocyte differentiation during skeletal development, postnatal growth, and fracture repair. We found that *Yap1* regulates multiple steps in the chondrocyte lineage in which *Yap1* promotes early chondrocyte proliferation but inhibits subsequent chondrocyte maturation. As a result, endochondral ossification is inhibited. Strikingly, bone repair is remarkably impaired that most of the chondrocytes are maintained at an immature state in the cartilaginous callus tissues.

It is interesting that the function of *Yap1* in bone repair is much more significant than that of skeletal development and skeletal growth because the bone fracture phenotypes were already very obvious when using the heterozygous *Col2a1-Yap1*$^{tg/+}$ transgenic mice. In contrast, only homozygous *Col2a1-Yap1*$^{tg/tg}$ transgenic mice demonstrated severe bone defects during skeletal development and growth. These results indicate that *Yap1* plays a more prominent role during bone regeneration and repair. The discrepancies of the phenotypes of *Yap1* overexpression between bone repair and skeletal development can be reconciled by the fact that many other signaling pathways are highly active during embryonic bone development (Long and Ornitz, 2013). For instance, Ihh and Pthlh signaling (St-Jacques et al., 1999; Vortkamp et al., 1996) play major roles to control the pace of chondrocyte proliferation, hypertrophy, and maturation during endochondral bone formation. However, these signaling activities gradually reduce after birth (Mak et al., 2008a; Tsukazaki et al., 1995). In contrast, the expression and activities of Hippo core components such as Lats and Msts gradually increase along with bone maturation (Song et al., 2012) suggesting that Hippo signaling is more important in regulating adult bone homeostasis. Consistently, we also observed that endogenous expression of Yap1 is reduced after birth (Figure 1B). Thus, Mst kinases should be constitutively active to suppress *Yap1* functions in postnatal bone homeostasis. Therefore, overexpression of *Yap1* during bone repair resulted in a more pronounced phenotype than that of skeletal development.

In fact, the overall inhibitory function of *Yap1* in skeletal development and callus formation is somewhat paradoxical to its role in promoting cell growth and survival as in many soft tissues as

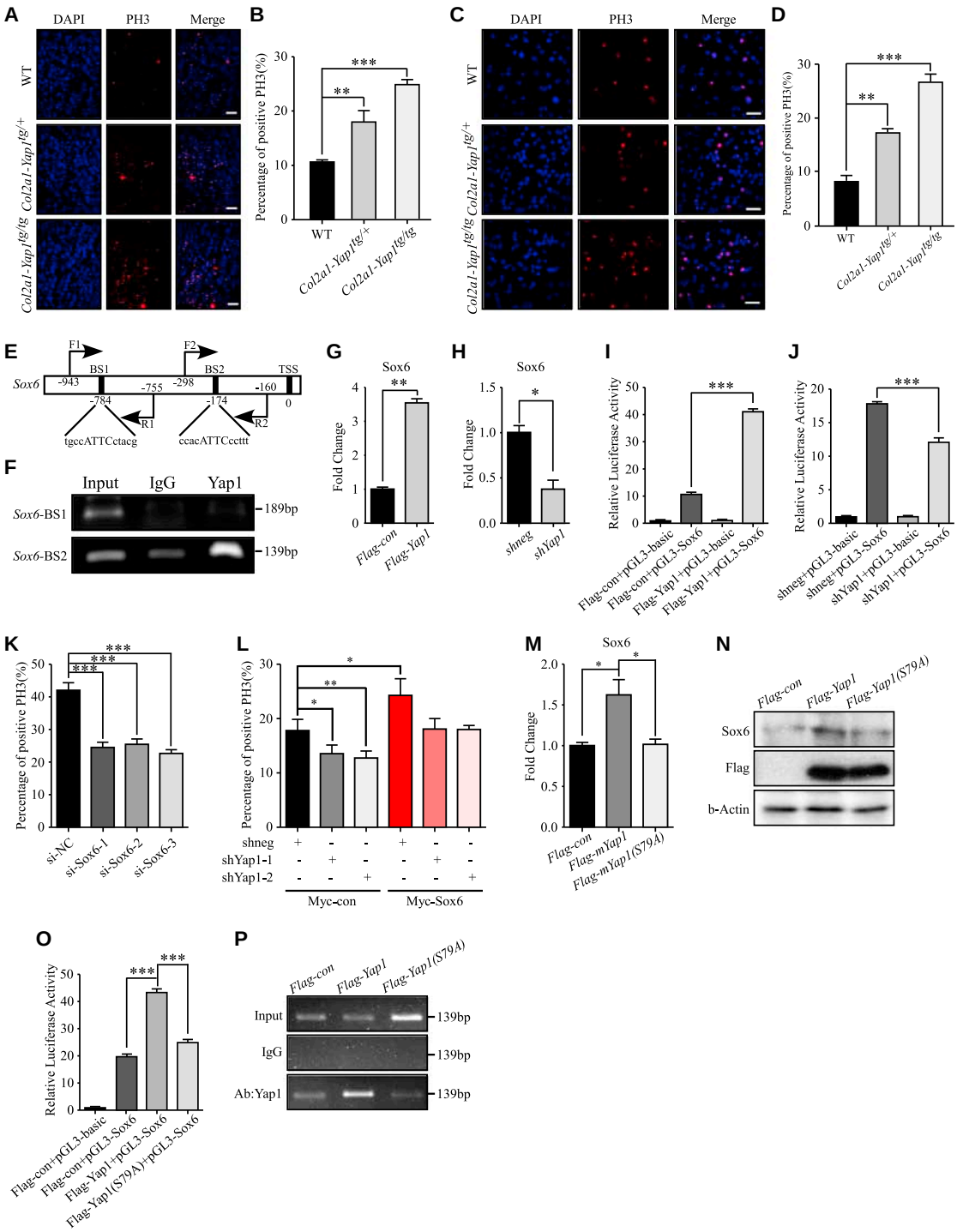

Figure 5. *Sox6* Is a Direct Target of *Yap1* in Promoting Chondrocyte Proliferation

(A) Fluorescent immunohistochemistry of phosphohistone-3 (PH3) of tibial growth plates of respective mice at day 1 as shown (n = 3 per group). Scale bars, 250 μm.

(B) Statistical analysis of PH3 positive cells in (A).

(C) PH3 staining using primary chondrocytes isolated from respective mice as shown. Scale bars, 50 μm.

(D) Statistical analysis of PH3 positive cells in (C).

(E) Schematic diagram of tentative *Teads* binding sites in the *Sox6* promoter (TSS, transcription start site; BS, binding site).

(legend continued on next page)

well as during tumorigenesis. We demonstrate that Yap1 promotes early chondrocyte proliferation, which is consistent to its known functions as in other cell contexts in soft tissues. However, the increase of extracellular matrix (ECM) stiffness in cartilage tissues may affect the functional outcomes mediated by *Yap1*. It has been reported that ECM stiffness regulates *Yap1* activity (Dupont et al., 2011) and *Yap1* is also required for cell-cell contact inhibition (Zhao et al., 2007). The highly rigid skeletal environment may therefore interfere with the cellular responses of *Yap1* activities, which results in different phenotypic outcomes in the skeletal tissues, which lead to inhibition of chondrocyte maturation. In addition, previous study also demonstrates that *Yap1* can function as a suppressor of *Osteocalcin* activation in osseous cells (Zaidi et al., 2004). Given the highly related lineages of chondrocytes and osteoblasts in the skeletal system, it is not surprising that *Yap1* employs similar mechanisms in regulating chondrocyte maturation by suppression of *Col10a1* expression. However, the upstream signaling cascades that regulate *Yap1* activities are different. Our work here demonstrates a possible role of Hippo pathway mediated by *Yap1* in chondrocyte differentiation because the *Mst1*$^{c/c}$*; Mst2*$^{c/c}$*; Dermo1-Cre* mutant mice also display similar phenotypes as the *Col2a1-Yap1*$^{tg/+}$ transgenic mice. However, the phenotypes from the *Mst1*$^{c/c}$*; Mst2*$^{c/c}$*; Dermo1-Cre* mutant mice was more severe, which can be accounted for by the fact that not only chondrocyte lineage was being affected, but Mst1/2 inactivation in the osteoblast lineage may also have contributed to the phenotypes.

Apart from chondrocyte differentiation, *Yap1* also determines alternate cell-fate choices between osteogenesis and adipogenesis from MSCs (Seo et al., 2013). Both *Yap1* knockdown and *Yap1* overexpression impair adipogenesis. However, Yap1 overexpression blocks osteogenesis through binding to β-catenin and induces Wnt antagonist Dkk1. In line with this, our work here also demonstrates that the level of *Yap1* has to be exquisitely controlled in the chondrocyte lineage for proper chondrocyte differentiation since *Yap1* regulates both chondrocyte proliferation and hypertrophy simultaneously. It is important to note that, other than *Yap1*, its close paralog *Taz* is also an effector of Hippo pathway. *Taz* co-activates *Runx2*-dependent gene transcription to promote osteogenesis and suppresses *Pparγ* to inhibit adipogenesis (Cui et al., 2003; Hong et al., 2005). We showed that *Taz* similarly promotes chondroprogenitor cell proliferation as *Yap1*. However, *Taz* function in opposite with *Yap1* in regulating chondrocyte maturation. It remains unclear how Hippo signaling precisely coordinates the differential effects of *Yap1* and *Taz* in the regulation of chondro, osteo, and adipo lineages. It is interesting to further investigate the interplay between *Yap1* and *Taz* in regulating cell-fate commitment. To conclude, our work identifies mechanistic functions of *Yap1* in regulating chondrocyte differentiation and, in particular, its prominent effect during bone repair, which may be implicated for the development of therapeutics for fracture healing.

EXPERIMENTAL PROCEDURES

Generation of Mouse Strains

The *Mst1* (Lu et al., 2010; Song et al., 2010), *Mst2* (Lu et al., 2010; Song et al., 2010), *Yap1* (Xin et al., 2011; Zhang et al., 2010), *Col2a1-Cre* (Ovchinnikov et al., 2000), and *Dermo1-Cre* (Yu et al., 2003) mouse lines have been described previously. *Col2a1-Yap1*$^{tg/+}$ transgenic lines were generated (C57Bl6 × CBA) using *Col2a1* promoter and enhancer as described (Long et al., 2001). Full-length mouse *Yap1* cDNA (isform2) was cloned under the control of the *Col2a1* promoter and enhancer. Two independent transgenic lines were generated by pronuclear injection. The line TG01 with the highest expression of *Yap1* in the cartilage was selected for most of the studies. Homozygous *Col2a1-Yap1*$^{tg/tg}$ transgenic line was generated by self-crossing TG01 heterozygous transgenic mice, which gave rise to a more severe phenotype. Genotyping was done by PCR using genomic DNA isolated from the tail tips. All animal experiments were performed according to procedures approved by the Animal Experimentation Ethics Committee of the Chinese University of Hong Kong.

Plasmid Construction

Full-length mouse *Yap1* cDNA (isform2) was subcloned into *pFLAG* (*pCMV-Tag 2C*, Stratagene), *pCDH* (*pCDH-CMV-MCS*, SBI System Biosciences), *pEGFP-C1* (Invitrogen), and *pAd Track* (*pAdTrack-CMV*, Addgene) vectors, respectively. Full-length *Taz* and *Runx2* were subcloned into *pFLAG* (*pCMV-Tag 2C*, Stratagene). Full-length *Sox6* and *Tead1* were subcloned into *pCDNA3.1 Myc-His(–)* (Invitrogen) vectors. For *shRNA* plasmid construction, two different pairs of oligos containing complementary hairpin sequences were synthesized and cloned into *pLV-3* (*pGLVH1/GFP+Puro*, GenePharma) lentiviral vector. The targeted sequences for *Yap1* gene were 5′-GGCAA TACGGAATATCAAT-3′ and 5′-GCGCTGAGTTCCGAAATCT-3′, respectively.

Skeletal Preparation, X-Ray Analyses and Micro-computed Tomography Analysis

Embryos and newborns were skinned, eviscerated, and fixed in 4% paraformaldehyde. Skeletal preparation was performed as described (McLeod, 1980). For X-ray analyses, mice were anesthetized and radiographed using the Faxitron MX-20 Digital machine (Faxitron X-Ray) at 32 kV for 6,000 ms. Micro-CT analyses were performed using μCT40 (Scanco Medical) with a resolution of 8 μm isometric voxel with 70 kV and 114 μA. Three-dimensional (3D) reconstruction was performed for the regions of interest (ROIs) and subjected to bone microarchitecture and mineral density analyses using built-in software from Scanco Medical and published protocol (Zhang et al., 2012).

Bone Fracture Model

Unilateral fractures were produced in the right femora as previously described (Lindsey et al., 2010). Briefly, the mice were anesthetized and the hindquarter

(F) ChIP assay using primary chondrocytes isolated from the *Col2a1-Yap1*$^{tg/+}$ transgenic mice. PCR was performed using primers (F1-R1 and F2-R2) flanking the tentative *Teads* binding sites of the promoters as shown in (E). See also Figure S4.
(G and H) *Sox6* expression in primary chondrocytes with (G) *Yap1* overexpression or (H) *Yap1* knockdown.
(I and J) Dual luciferase assay of *Sox6* activities using reporter plasmids of Sox6 promoter (1.2 kb) in primary chondrocytes with (I) *Yap1* overexpression and (J) *Yap1* knockdown.
(K) Statistical analysis of cell proliferation in *Col2a1-Yap1* chondrocytes after *Sox6* knockdown.
(L) Statistical analysis of chondrocyte proliferation with *Yap1* knockdown and *Sox6* overexpression.
(M and N) RNA (M) and protein (N) analysis of *Sox6* expression with wild-type mouse *Yap1* and *Yap1(S79A)*.
(O) Luciferase analysis with *Yap1(S79A)*.
(P) ChIP assay with *Yap1(S79A)* expression. Samples were collected in triplicates, and three independent experiments were performed.
Error bars represent SD (***p < 0.001; **p < 0.01; *p < 0.05).

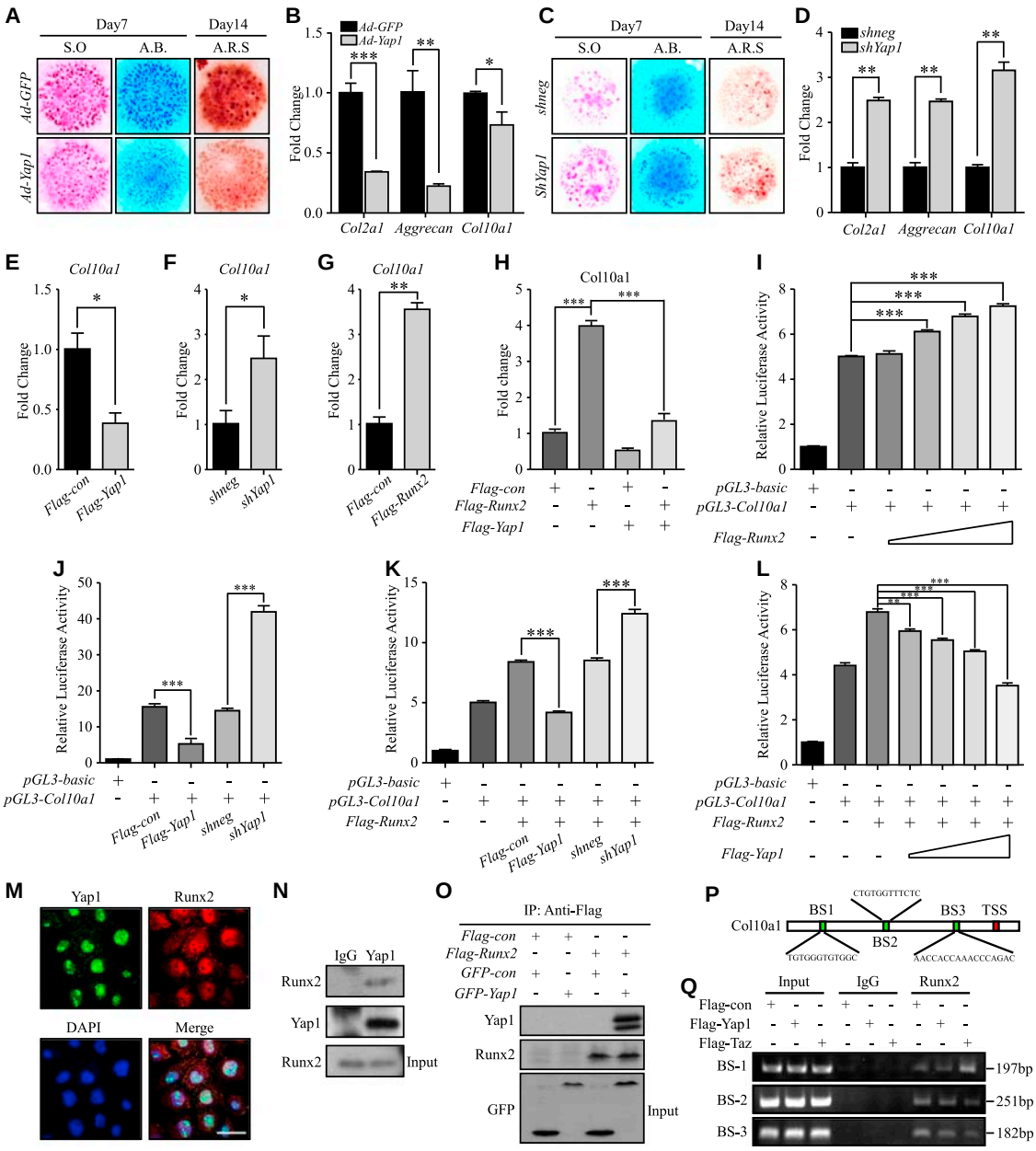

Figure 6. *Yap1* Inhibits Chondrocyte Maturation by Regulating *Col10a1* Expression

(A) Micromass culture using limb buds isolated from wild-type mice at E12.5 with *Yap1* overexpression (A.B., Alcian blue; S.O., Safranin O; A.R.S., Alizarin Red S staining). See also Figure S5.

(B) Gene expression analysis using RNA isolated at day 7 from (A).

(C) Micromass culture of with *Yap1* knockdown.

(D) Gene expression analysis using RNA isolated at day 7 from (C).

(E and F) *Col10a1* expression in primary chondrocytes with *Yap1* manipulation as shown.

(G) *Col10a1* expression in primary chondrocytes with *Runx2* overexpression.

(H–L) Dual luciferase assay of *Col10a1* activities using reporter plasmids with 1.5-kb *Col10a1* promoter region in primary chondrocytes. See also Figure S6.

(M) Immunofluorescence of primary chondrocytes with Yap1 (green) and Runx2 (red). Scale bar, 30 μm.

(N and O) Immunoprecipitation analysis with (N) Yap1 antibodies and (O) anti-Flag antibodies for pull-down of Runx2 in primary chondrocytes.

(P) Schematic diagram of *Runx2* binding domains in the *Col10a1* promoter (TSS, transcription start site; BS, binding site).

(Q) ChIP assay in primary chondrocytes using Runx2 antibodies. Each assay was performed in triplicates and repeated for three times independently. Error bars represent SD (***p < 0.001; **p < 0.01; *p < 0.05).

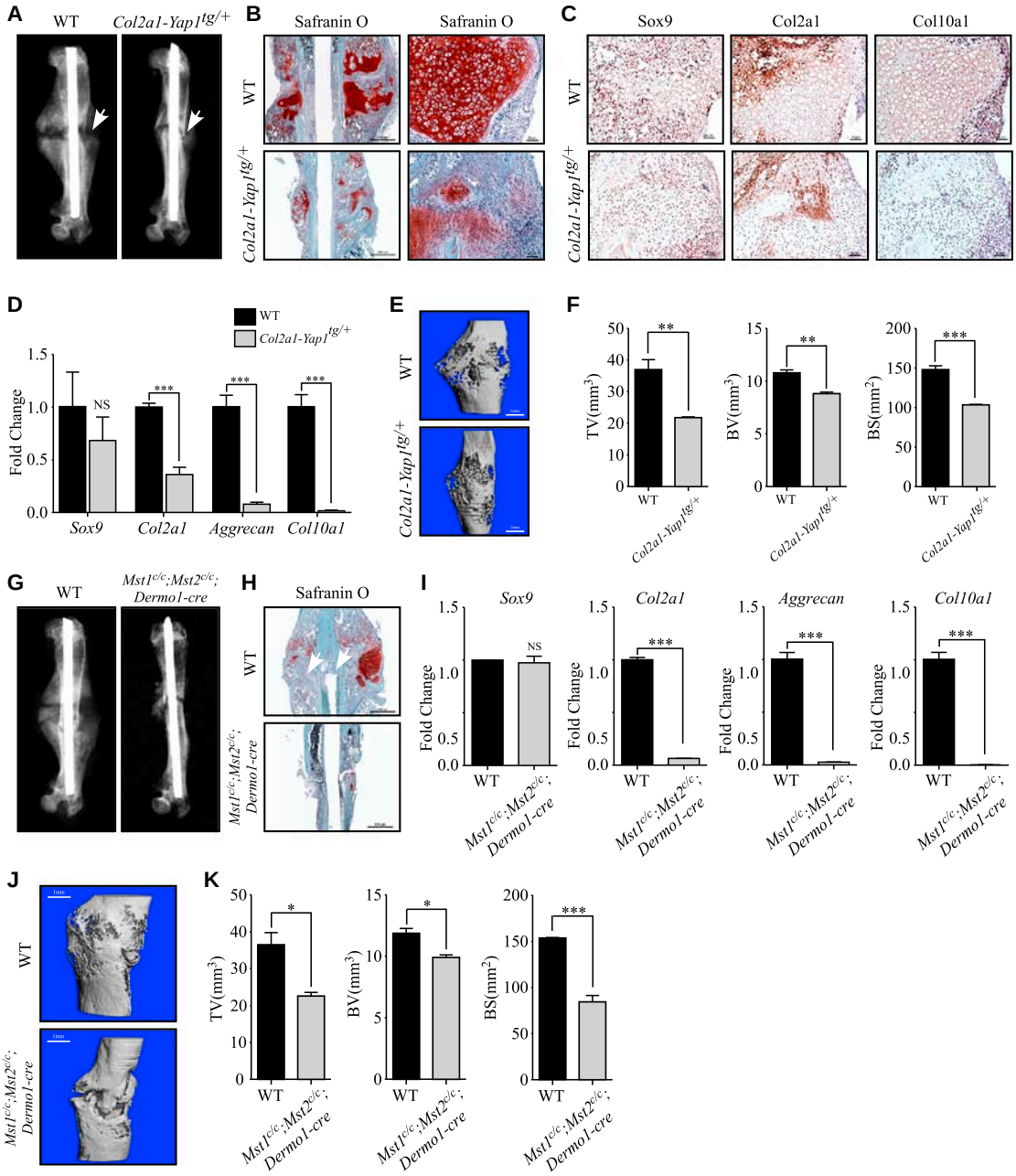

Figure 7. Fracture Healing Is Impaired in the *Col2a1-Yap1*$^{tg/+}$ Transgenic Mice and the *Mst1*$^{c/c}$; *Mst2*$^{c/c}$; *Dermo1-Cre* Mutant Mice

(A) X-ray analysis of fractured femora of 3-month-old transgenic mice 2 weeks after fracture injury on the right hind limbs (n = 6 per group). White arrows point to the fracture site where soft callus tissues formed. See also Figure S7.

(B) Safranin O staining of the fracture sites at 2 weeks after injury (n = 6 per group). Scale bars, 1,000 μm (left panel); 60 μm (right panel).

(C) Immunohistochemistry of chondrocyte markers in the callus tissues of respective mice (n = 3 per group) 2 weeks after fracture injuries as shown. Scale bars, 60 μm.

(D) Gene expression analysis using tissues isolated from (B). qRT-PCR analysis was performed in triplicates and repeated three times independently.

(E) 3D micro-CT images of the callus tissues at the fracture sites 4 weeks after surgery (n = 3 per group). Scale bars, 1 mm.

(F) Microarchitecture analysis of bone parameters from (E).

(G–K) Similar analysis using the *Mst1*$^{c/c}$; *Mst2*$^{c/c}$; *Dermo1-Cre* mutant mice as shown in (A)–(F).

Error bars represent SD (***p < 0.001; **p < 0.01; *p < 0.05; NS, not significant).

Please cite this article in press as: Deng et al., Yap1 Regulates Multiple Steps of Chondrocyte Differentiation during Skeletal Development and Bone Repair, Cell Reports (2016), http://dx.doi.org/10.1016/j.celrep.2016.02.021

was shaved. The leg was fractured using a blunted blade placed at the mid-shaft of the femur. Following fracture, an incision was made on the dorsolateral surface of the femur from the area of the greater trochanter to the epicondyles of the femur through the gluteus superficialis. The two ends of the fractured femur were fixed using a 23G needle. The wound was closed using Polysorb for myofascial closure and staples for skin closure. The animals were randomly assigned to surgical groups, but they were not conducted in a completely blinded fashion. We surgically fractured 12-week-old female wild-type mice, age- and sex-matched *Col2a1-Yap1*$^{tg/+}$ transgenic mice, and *Mst1*$^{c/c}$*; Mst2*$^{c/c}$*; Dermo1-Cre* mutant mice, respectively, for bone repair analyses. The fracture protocol was approved according to the Animals Ordinance Chapter 340 ([13-392] in DH/HA&P/8/2/1 Pt.32)). At 2 weeks post-operation, mice were anesthetized and radiographed to examine cartilaginous callus formation. Six mice per group were used for X-ray and histological analyses, respectively. Three mice per group were used for RNA extraction and gene expression analyses. At 4 weeks post-operation, three mice per group were used for micro-CT analyses.

Histological Analyses and Western Blots

Primary antibodies used in immunohistochemistry and immunofluorescence include Phospho-histone H3 (PH3) antibodies (Santa Cruz Biotechnology, sc-8656-R) at 1:100, Yap1 antibodies (Cell Signaling Technology, 4912s) at 1:50, p-Yap1 antibodies (Cell Signal, 4911s) at 1:50, Sox9 antibodies (Abcam, ab3697) at 1:50, Col2a1 antibodies (Santa Cruz, sc-28887) at 1:100, Mmp13 antibodies (Abcam, ab39012) at 1:50, Col10a1 antibodies (Abcam, ab58632) at 1:50 and Runx2 antibodies (Cell Signal, 8486S) at 1:50. The immunohistochemistry was performed using Histostain-*Plus* IHC kit (Invitrogen) following the manufacturer's protocol. For western blot analysis, β-Actin antibodies (Santa Cruz, sc-130656) at 1:2,000 were used for normalization, Yap1 antibodies (Cell Signal, 4912s) at 1:1000, p-Yap1 antibodies (Cell Signal, 4911s) at 1:1,000, Runx2 antibodies (Cell Signal, 8486S) at 1:1000, Taz antibodies (BD Pharmingen, 560235) at 1:1,000, and GFP antibodies (Abcam, ab290) at 1:2,000 were used. Procedures were followed as previously described (Topol et al., 2003). Anti-Flag M2 affinity gel (Sigma, A2220) was used for immunoprecipitation.

Colony Formation Assay

5,000 cells were seeded in 60-mm culture dish and cultured for 5 days. Crystal violet staining was performed for counting the colony number. Triplicate plates were counted.

Micromass Culture and Isolation of Primary Chondrocytes

Micromass cultures were performed as previously described (Guo et al., 2004). *Yap1 adenovirus* was used to infect the cells for at least 4 hr before seeding into culture wells. *GFP-adenovirus* was used for comparison. Primary chondrocytes were isolated from the ventral parts of the rib cages of 0- to 3-day-old wild-type and transgenic pups as described (Mak et al., 2008b).

Chromatin Immunoprecipitation

Primary chondrocytes (1×10^7 cells) were fixed with 1% formaldehyde directly in culture medium at 37°C for 10 min. Cells were subsequently quenched by glycine with final concentration of 125 mM for 5 min at room temperature. Cells were washed and lysed before sonication. Samples were sonicated for ten cycles of 10 s each to generate an average DNA fragment size of about 500 bp. Immunoprecipitation was performed following standard protocols as described previously (Nelson et al., 2006) with Yap1 antibodies (Cell Signal, 4912s) at 1:100, Runx2 antibodies (Cell Signal, 8486S) at 1:100 or 5 μg rabbit normal immunoglobulin G (IgG) (Cell Signal, 2729). ChIP grade protein A/G agarose was used (Thermo Scientific, 26159).

RNA Isolation and qRT-PCR

Total RNA was isolated using the TRIzol reagent (Invitrogen) according to the manufacturer's instructions. Reverse transcription was performed using M-MLV reverse Transcriptase (Invitrogen). qPCR was carried out using a Platinum SYBR Green kit (Applied Biosystems). Samples were normalized with *Gapdh*. Fold difference was determined by $2^{-\Delta\Delta CT}$ methods.

Dual Luciferase Assay

Primary chondrocytes were transfected with either *pGL3-basic*, *pGL3-Sox6* (1.2 kb), or *pGL3-Col10a1* (1.5 kb) luciferase reporters together with *Flag-con*, *Flag-Yap1*, *Flag-Runx2*, *Flag-Taz*, *shneg*, or *shYap1* using Lipofectamine 3000 (Invitrogen). *pRL-TK* vector (Promega) with *Renilla* was co-transfected as reference controls. Cells were subjected to luciferase activity measurement as described in dual luciferase reporter assay kit (Promega).

Statistical Analyses

Two-tailed Student's t test was used for comparison between two groups as shown by brackets. Results are represented as mean ± SD. p values <0.05 were considered to be significant. No significant differences in variance between groups were detected. All analyses were performed with GraphPad Prism software (v.5.0). No statistical method was used to predetermine sample size. The inclusion criteria were the appropriate genotype of the mice.

SUPPLEMENTAL INFORMATION

Supplemental Information includes Supplemental Experimental Procedures, seven figures, and one table and can be found with this article online at http://dx.doi.org/10.1016/j.celrep.2016.02.021.

AUTHOR CONTRIBUTIONS

Y.D. designed and performed most of the experiments; P.L. generated animal models; G.L. contributed to X-ray analysis; L.Q. contributed to Micro-CT analysis; H.S. and A.W. contributed to *Yap1* cKO mutant analysis; K.K.M. analyzed, interpreted data, and supervised the project; Y.D. and K.K.M. wrote the manuscript.

ACKNOWLEDGMENTS

We thank members of K.K.M.'s lab for stimulating discussions. This work is supported by the Seed Fund of the School of Biomedical Sciences, The Chinese University of Hong Kong (4620504), Direct grant for research from Research Grant Council, Hong Kong (CUHK2041745), Guangdong Science and Technology Bureau International Science and Technology Collaboration Program (20130501c), and a donation by Lui Che Woo Foundation Limited to K.K.M. and the Fundamental Research Funds for the Central Universities (2014QN81003) to H.S.

Received: June 22, 2015
Revised: January 3, 2016
Accepted: January 29, 2016
Published: February 25, 2016

REFERENCES

Akiyama, H., Chaboissier, M.C., Martin, J.F., Schedl, A., and de Crombrugghe, B. (2002). The transcription factor Sox9 has essential roles in successive steps of the chondrocyte differentiation pathway and is required for expression of Sox5 and Sox6. Genes Dev. *16*, 2813–2828.

Alarcón, C., Zaromytidou, A.I., Xi, Q., Gao, S., Yu, J., Fujisawa, S., Barlas, A., Miller, A.N., Manova-Todorova, K., Macias, M.J., et al. (2009). Nuclear CDKs drive Smad transcriptional activation and turnover in BMP and TGF-beta pathways. Cell *139*, 757–769.

Bolander, M.E. (1992). Regulation of fracture repair by growth factors. Proc. Soc. Exp. Biol. Med. *200*, 165–170.

Bruder, S.P., Fink, D.J., and Caplan, A.I. (1994). Mesenchymal stem cells in bone development, bone repair, and skeletal regeneration therapy. J. Cell. Biochem. *56*, 283–294.

Cui, C.B., Cooper, L.F., Yang, X., Karsenty, G., and Aukhil, I. (2003). Transcriptional coactivation of bone-specific transcription factor Cbfa1 by TAZ. Mol. Cell. Biol. *23*, 1004–1013.

Deschaseaux, F., Sensébé, L., and Heymann, D. (2009). Mechanisms of bone repair and regeneration. Trends Mol. Med. *15*, 417–429.

Dupont, S., Morsut, L., Aragona, M., Enzo, E., Giulitti, S., Cordenonsi, M., Zanconato, F., Le Digabel, J., Forcato, M., Bicciato, S., et al. (2011). Role of YAP/TAZ in mechanotransduction. Nature *474*, 179–183.

Einhorn, T.A. (1998). The cell and molecular biology of fracture healing. Clin. Orthop. Relat. Res. (*355, Suppl*), S7–S21.

Ellegaard, M., Jørgensen, N.R., and Schwarz, P. (2010). Parathyroid hormone and bone healing. Calcif. Tissue Int. *87*, 1–13.

Espanel, X., and Sudol, M. (2001). Yes-associated protein and p53-binding protein-2 interact through their WW and SH3 domains. J. Biol. Chem. *276*, 14514–14523.

Ferguson, C., Alpern, E., Miclau, T., and Helms, J.A. (1999). Does adult fracture repair recapitulate embryonic skeletal formation? Mech. Dev. *87*, 57–66.

Fernandez-L, A., Northcott, P.A., Dalton, J., Fraga, C., Ellison, D., Angers, S., Taylor, M.D., and Kenney, A.M. (2009). YAP1 is amplified and up-regulated in hedgehog-associated medulloblastomas and mediates Sonic hedgehog-driven neural precursor proliferation. Genes Dev. *23*, 2729–2741.

Guo, X., Day, T.F., Jiang, X., Garrett-Beal, L., Topol, L., and Yang, Y. (2004). Wnt/beta-catenin signaling is sufficient and necessary for synovial joint formation. Genes Dev. *18*, 2404–2417.

Halder, G., and Johnson, R.L. (2011). Hippo signaling: growth control and beyond. Development *138*, 9–22.

Han, Y., and Lefebvre, V. (2008). L-Sox5 and Sox6 drive expression of the aggrecan gene in cartilage by securing binding of Sox9 to a far-upstream enhancer. Mol. Cell. Biol. *28*, 4999–5013.

Heallen, T., Morikawa, Y., Leach, J., Tao, G., Willerson, J.T., Johnson, R.L., and Martin, J.F. (2013). Hippo signaling impedes adult heart regeneration. Development *140*, 4683–4690.

Hong, J.H., Hwang, E.S., McManus, M.T., Amsterdam, A., Tian, Y., Kalmukova, R., Mueller, E., Benjamin, T., Spiegelman, B.M., Sharp, P.A., et al. (2005). TAZ, a transcriptional modulator of mesenchymal stem cell differentiation. Science *309*, 1074–1078.

Huang, Y., Zhang, X., Du, K., Yang, F., Shi, Y., Huang, J., Tang, T., Chen, D., and Dai, K. (2012). Inhibition of beta-catenin signaling in chondrocytes induces delayed fracture healing in mice. J. Orthop. Res. *30*, 304–310.

Karpowicz, P., Perez, J., and Perrimon, N. (2010). The Hippo tumor suppressor pathway regulates intestinal stem cell regeneration. Development *137*, 4135–4145.

Kronenberg, H.M. (2003). Developmental regulation of the growth plate. Nature *423*, 332–336.

Lefebvre, V., and de Crombrugghe, B. (1998). Toward understanding SOX9 function in chondrocyte differentiation. Matrix Biol. *16*, 529–540.

Lefebvre, V., Li, P., and de Crombrugghe, B. (1998). A new long form of Sox5 (L-Sox5), Sox6 and Sox9 are coexpressed in chondrogenesis and cooperatively activate the type II collagen gene. EMBO J. *17*, 5718–5733.

Li, F., Lu, Y., Ding, M., Napierala, D., Abbassi, S., Chen, Y., Duan, X., Wang, S., Lee, B., and Zheng, Q. (2011). Runx2 contributes to murine Col10a1 gene regulation through direct interaction with its cis-enhancer. J. Bone Miner. Res. *26*, 2899–2910.

Lindsey, B.A., Clovis, N.B., Smith, E.S., Salihu, S., and Hubbard, D.F. (2010). An animal model for open femur fracture and osteomyelitis: Part I. J. Orthop. Res. *28*, 38–42.

Long, F., and Ornitz, D.M. (2013). Development of the endochondral skeleton. Cold Spring Harb. Perspect. Biol. *5*, a008334.

Long, F., Zhang, X.M., Karp, S., Yang, Y., and McMahon, A.P. (2001). Genetic manipulation of hedgehog signaling in the endochondral skeleton reveals a direct role in the regulation of chondrocyte proliferation. Development *128*, 5099–5108.

Lu, L., Li, Y., Kim, S.M., Bossuyt, W., Liu, P., Qiu, Q., Wang, Y., Halder, G., Finegold, M.J., Lee, J.S., and Johnson, R.L. (2010). Hippo signaling is a potent in vivo growth and tumor suppressor pathway in the mammalian liver. Proc. Natl. Acad. Sci. USA *107*, 1437–1442.

Mak, K.K., Bi, Y., Wan, C., Chuang, P.T., Clemens, T., Young, M., and Yang, Y. (2008a). Hedgehog signaling in mature osteoblasts regulates bone formation and resorption by controlling PTHrP and RANKL expression. Dev. Cell *14*, 674–688.

Mak, K.K., Kronenberg, H.M., Chuang, P.T., Mackem, S., and Yang, Y. (2008b). Indian hedgehog signals independently of PTHrP to promote chondrocyte hypertrophy. Development *135*, 1947–1956.

McLeod, M.J. (1980). Differential staining of cartilage and bone in whole mouse fetuses by alcian blue and alizarin red S. Teratology *22*, 299–301.

Nelson, J.D., Denisenko, O., and Bomsztyk, K. (2006). Protocol for the fast chromatin immunoprecipitation (ChIP) method. Nat. Protoc. *1*, 179–185.

Ovchinnikov, D.A., Deng, J.M., Ogunrinu, G., and Behringer, R.R. (2000). Col2a1-directed expression of Cre recombinase in differentiating chondrocytes in transgenic mice. Genesis *26*, 145–146.

Pan, D. (2007). Hippo signaling in organ size control. Genes Dev. *21*, 886–897.

Pan, D. (2010). The hippo signaling pathway in development and cancer. Dev. Cell *19*, 491–505.

Rosenbluh, J., Nijhawan, D., Cox, A.G., Li, X., Neal, J.T., Schafer, E.J., Zack, T.I., Wang, X., Tsherniak, A., Schinzel, A.C., et al. (2012). β-Catenin-driven cancers require a YAP1 transcriptional complex for survival and tumorigenesis. Cell *151*, 1457–1473.

Seo, E., Basu-Roy, U., Gunaratne, P.H., Coarfa, C., Lim, D.S., Basilico, C., and Mansukhani, A. (2013). SOX2 regulates YAP1 to maintain stemness and determine cell fate in the osteo-adipo lineage. Cell Rep. *3*, 2075–2087.

Smits, P., Li, P., Mandel, J., Zhang, Z., Deng, J.M., Behringer, R.R., de Crombrugghe, B., and Lefebvre, V. (2001). The transcription factors L-Sox5 and Sox6 are essential for cartilage formation. Dev. Cell *1*, 277–290.

Song, H., Mak, K.K., Topol, L., Yun, K., Hu, J., Garrett, L., Chen, Y., Park, O., Chang, J., Simpson, R.M., et al. (2010). Mammalian Mst1 and Mst2 kinases play essential roles in organ size control and tumor suppression. Proc. Natl. Acad. Sci. USA *107*, 1431–1436.

Song, H., Kim, H., Lee, K., Lee, D.H., Kim, T.S., Song, J.Y., Lee, D., Choi, D., Ko, C.Y., Kim, H.S., et al. (2012). Ablation of Rassf2 induces bone defects and subsequent haematopoietic anomalies in mice. EMBO J. *31*, 1147–1159.

St-Jacques, B., Hammerschmidt, M., and McMahon, A.P. (1999). Indian hedgehog signaling regulates proliferation and differentiation of chondrocytes and is essential for bone formation. Genes Dev. *13*, 2072–2086.

Takeda, S., Bonnamy, J.P., Owen, M.J., Ducy, P., and Karsenty, G. (2001). Continuous expression of Cbfa1 in nonhypertrophic chondrocytes uncovers its ability to induce hypertrophic chondrocyte differentiation and partially rescues Cbfa1-deficient mice. Genes Dev. *15*, 467–481.

Topol, L., Jiang, X., Choi, H., Garrett-Beal, L., Carolan, P.J., and Yang, Y. (2003). Wnt-5a inhibits the canonical Wnt pathway by promoting GSK-3-independent beta-catenin degradation. J. Cell Biol. *162*, 899–908.

Tsuji, K., Bandyopadhyay, A., Harfe, B.D., Cox, K., Kakar, S., Gerstenfeld, L., Einhorn, T., Tabin, C.J., and Rosen, V. (2006). BMP2 activity, although dispensable for bone formation, is required for the initiation of fracture healing. Nat. Genet. *38*, 1424–1429.

Tsukazaki, T., Ohtsuru, A., Enomoto, H., Yano, H., Motomura, K., Ito, M., Namba, H., Iwasaki, K., and Yamashita, S. (1995). Expression of parathyroid hormone-related protein in rat articular cartilage. Calcif. Tissue Int. *57*, 196–200.

Vassilev, A., Kaneko, K.J., Shu, H., Zhao, Y., and DePamphilis, M.L. (2001). TEAD/TEF transcription factors utilize the activation domain of YAP65, a Src/Yes-associated protein localized in the cytoplasm. Genes Dev. *15*, 1229–1241.

Vortkamp, A., Lee, K., Lanske, B., Segre, G.V., Kronenberg, H.M., and Tabin, C.J. (1996). Regulation of rate of cartilage differentiation by Indian hedgehog and PTH-related protein. Science *273*, 613–622.

Please cite this article in press as: Deng et al., Yap1 Regulates Multiple Steps of Chondrocyte Differentiation during Skeletal Development and Bone Repair, Cell Reports (2016), http://dx.doi.org/10.1016/j.celrep.2016.02.021

Vortkamp, A., Pathi, S., Peretti, G.M., Caruso, E.M., Zaleske, D.J., and Tabin, C.J. (1998). Recapitulation of signals regulating embryonic bone formation during postnatal growth and in fracture repair. Mech. Dev. *71*, 65–76.

Wang, H.L., and Boyapati, L. (2006). "PASS" principles for predictable bone regeneration. Implant Dent. *15*, 8–17.

Wu, S., Huang, J., Dong, J., and Pan, D. (2003). hippo encodes a Ste-20 family protein kinase that restricts cell proliferation and promotes apoptosis in conjunction with salvador and warts. Cell *114*, 445–456.

Xin, M., Kim, Y., Sutherland, L.B., Qi, X., McAnally, J., Schwartz, R.J., Richardson, J.A., Bassel-Duby, R., and Olson, E.N. (2011). Regulation of insulin-like growth factor signaling by Yap governs cardiomyocyte proliferation and embryonic heart size. Sci. Signal. *4*, ra70.

Yu, K., Xu, J., Liu, Z., Sosic, D., Shao, J., Olson, E.N., Towler, D.A., and Ornitz, D.M. (2003). Conditional inactivation of FGF receptor 2 reveals an essential role for FGF signaling in the regulation of osteoblast function and bone growth. Development *130*, 3063–3074.

Zaidi, S.K., Sullivan, A.J., Medina, R., Ito, Y., van Wijnen, A.J., Stein, J.L., Lian, J.B., and Stein, G.S. (2004). Tyrosine phosphorylation controls Runx2-mediated subnuclear targeting of YAP to repress transcription. EMBO J. *23*, 790–799.

Zhang, N., Bai, H., David, K.K., Dong, J., Zheng, Y., Cai, J., Giovannini, M., Liu, P., Anders, R.A., and Pan, D. (2010). The Merlin/NF2 tumor suppressor functions through the YAP oncoprotein to regulate tissue homeostasis in mammals. Dev. Cell *19*, 27–38.

Zhang, G., Guo, B., Wu, H., Tang, T., Zhang, B.T., Zheng, L., He, Y., Yang, Z., Pan, X., Chow, H., et al. (2012). A delivery system targeting bone formation surfaces to facilitate RNAi-based anabolic therapy. Nat. Med. *18*, 307–314.

Zhao, B., Wei, X., Li, W., Udan, R.S., Yang, Q., Kim, J., Xie, J., Ikenoue, T., Yu, J., Li, L., et al. (2007). Inactivation of YAP oncoprotein by the Hippo pathway is involved in cell contact inhibition and tissue growth control. Genes Dev. *21*, 2747–2761.

Zhao, B., Li, L., Lei, Q., and Guan, K.L. (2010). The Hippo-YAP pathway in organ size control and tumorigenesis: an updated version. Genes Dev. *24*, 862–874.

Zhao, B., Tumaneng, K., and Guan, K.L. (2011). The Hippo pathway in organ size control, tissue regeneration and stem cell self-renewal. Nat. Cell Biol. *13*, 877–883.

Zheng, Q., Zhou, G., Morello, R., Chen, Y., Garcia-Rojas, X., and Lee, B. (2003). Type X collagen gene regulation by Runx2 contributes directly to its hypertrophic chondrocyte-specific expression in vivo. J. Cell Biol. *162*, 833–842.

Zhou, D., Conrad, C., Xia, F., Park, J.S., Payer, B., Yin, Y., Lauwers, G.Y., Thasler, W., Lee, J.T., Avruch, J., and Bardeesy, N. (2009). Mst1 and Mst2 maintain hepatocyte quiescence and suppress hepatocellular carcinoma development through inactivation of the Yap1 oncogene. Cancer Cell *16*, 425–438.